Lung Cancer Proliferation Correlates with [F-18]Fluorodeoxyglucose Uptake by Positron Emission Tomography[1]

Hubert Vesselle,[2] Rodney A. Schmidt, Jeffrey M. Pugsley, Melissa Li, Steve G. Kohlmyer, Eric Vallières, and Douglas E. Wood

Department of Radiology, Division of Nuclear Medicine [H. V., J. M. P., S. G. K.], Department of Pathology [R. A. S., M. L.], and Division of Thoracic Surgery [E. V., D. E. W.], University of Washington, Seattle, Washington 98195

ABSTRACT

Tumor proliferation has prognostic value in resected early-stage non-small cell lung cancer (NSCLC). We evaluated whether [F-18]fluorodeoxyglucose (FDG) uptake of NSCLC correlates with tumor proliferation and, thus, could noninvasively grade NSCLCs (refining patient prognosis and therapy). Thirty-nine patients with potentially resectable NSCLC underwent whole-body FDG positron emission tomography (PET) 45 min after i.v. injection of 10 mCi of FDG. Tumor FDG uptake was quantitated with the maximum pixel standardized uptake value (maxSUV). The lesion diameter from computed tomography was used to correct the maxSUV for partial volume effects using recovery coefficients determined for the General Electric Advance PET scanner. Thirty-eight patients underwent complete surgical staging (bronchoscopy and mediastinoscopy, with or without thoracotomy). One stage IV patient by PET underwent bronchoscopic biopsy only. Immunohistochemistry for Ki-67 (proliferation index marker) was performed on all of the 39 NSCLC specimens (35 resections, 1 percutaneous, and 3 surgical biopsies). The specimens were reviewed for cellular differentiation (poor, moderate, well) and tumor type. Lesions ranged from 0.7 to 6.1 cm. The correlation found between uncorrected maxSUV and lesion size (Rho, 0.56; $P = 0.0006$) disappeared when applying the recovery coefficients (Rho, −0.035; $P = 0.83$). Ki-67 expression (percentage of positive cells) correlated strongly with FDG uptake (corrected maxSUV: Rho, 0.73; $P < 0.0001$). The correlation was stronger for stage I lesions (11 stage IA, 15 stage IB): Rho, 0.79; $P < 0.0001$) and strongest in stage IB (Rho, 0.83; $P = 0.0019$). A significant association ($P < 0.0001$) between tumor differentiation and corrected SUV was noted. FDG PET may be used to noninvasively assess NSCLC proliferation *in vivo*, identifying rapidly growing NSCLCs with poor prognosis that could benefit from preoperative chemotherapy.

INTRODUCTION

Lung cancer is the leading cause of cancer death in the United States, with an estimated 171,600 new cases and 158,900 deaths in 1999 (1). NSCLC[3] accounts for approximately 80% of lung cancers and includes adenocarcinoma, squamous cell carcinoma, and large cell and mixed histologies.

Tumor stage and histopathological grade are used to describe the extent of disease and tumor aggressiveness. However, no comprehensive pathological grading system exists for all NSCLCs. Tumor stage is the strongest prognostic factor in NSCLC and the most important parameter that guides treatment decisions. Overall 5-year survival rates by pathological stage are: IA, 67%; IB, 57%; IIA, 55%; IIB, 38–39%; IIIA, 23–25%; IIIB, 3–7%; IV, 1% (2). Surgery represents the best chance for cure in NSCLC. However, surgery with curative intent is an option in only ~30% of cases [stages I, II, and selected IIIA ($T_3N_1M_0$)]. Even if a complete, presumably curative, resection can be performed, >50% will relapse, with the majority of these relapses occurring at distant sites (3–5). Hence, each pathological substage remains a heterogeneous population containing individuals at much higher risk of recurrence and death than others in the same substage. Therefore, there is a need for a noninvasive grading system to further characterize NSCLCs.

Measures of tumor proliferation have prognostic value in resected NSCLC (6–21). However, these markers require a biopsy or resection and are subject to tissue sampling errors. FDG uptake has been shown to correlate with tumor proliferative rates in lymphomas and in head and neck cancers (22–26). FDG uptake has also been shown to be a useful means of grading gliomas, head and neck cancers, lymphomas, breast cancer, and sarcomas (25, 27–35). Moreover, FDG uptake in focal pulmonary abnormalities has been shown to correlate with lesion doubling time (36), a measure previously shown to predict lung tumor aggressiveness (37–39). We therefore proposed to compare FDG uptake, quantitated as a SUV, with tumor proliferative rates assessed by immunohistochemistry (Ki-67

Received 5/19/00; accepted 7/6/00.
The costs of publication of this article were defrayed in part by the payment of page charges. This article must therefore be hereby marked *advertisement* in accordance with 18 U.S.C. Section 1734 solely to indicate this fact.
[1] This work was supported in part by NIH Grant 1R01 CA80907-01A1.
[2] To whom requests for reprints should be addressed, at Department of Radiology, Division of Nuclear Medicine, Box 356113, University of Washington Medical Center, 1959 North East Pacific Street, Seattle, WA 98195. Phone: (206) 598-4240; Fax: (206) 598-4496; E-mail: vesselle@u.washington.edu.

[3] The abbreviations used are: NSCLC, non-small cell lung cancer; PET, positron emission tomography; FDG, [F-18]fluorodeoxyglucose; FDGMR, FDG metabolic rate; SUV, standardized uptake value; maxSUV, (uncorrected lesion) maximum (pixel) SUV; gluc-PV corr maxSUV, glucose- and partial volume-corrected maxSUV; PV corr maxSUV, partial volume-corrected maxSUV; CT, computed tomography; ROI, region-of-interest; BSA, body surface area; PCNA, proliferating cell nuclear antigen; RC, recovery coefficient.

antigen score). Our hypothesis was that more metabolically active NSCLCs have higher proliferative rates (higher Ki-67 scores).

MATERIALS AND METHODS

Patient Selection

Thirty-nine patients with NSCLC were prospectively studied. All of the patients with potentially resectable NSCLC evaluated in the Thoracic Surgery Clinic at the University of Washington Medical Center between February 1998 and June 1999 underwent FDG PET imaging. Those who then underwent resection or surgical biopsy of their tumor were enrolled in this study, which was conducted under University of Washington Institutional Review Board approval. All of the patients had CT of the chest prior to FDG PET imaging. Lesion size was calculated by averaging all of the three lesion dimensions measured from the mediastinal windows of the CT scan and was used to correct SUV values for partial volume effects (see "Quantitative Imaging Analysis" below).

FDG PET Imaging

Imaging. All of the PET studies were performed on a General Electric Advance PET tomograph. FDG imaging was performed in all of the patients to quantitate FDG uptake as a proposed noninvasive measure of primary-tumor aggressiveness (tumor grade) and to localize other potential tumor sites as part of patient staging. Patients were asked to fast for 12 h prior to tracer administration. Two i.v. catheters were placed in opposite arms, one for tracer administration, the other for blood sampling. An initial blood sample was obtained at the time of i.v. catheter placement to screen for abnormally high plasma glucose levels. Just prior to tracer administration, patients also received 1 mg of i.v. lorazepam to decrease benign muscular uptake in the neck and upper thorax. Seven to 11 mCi of FDG was infused i.v. over a 2-min period using a Harvard pump (Harvard, Boston, MA). After a 45-min rest period, patients were placed supine in the scanner with the thorax positioned to fit within two contiguous 15-cm wide tomograph fields-of-view. Imaging always started with a 15-min-long emission scan performed over the thoracic field-of-view encompassing the primary lung cancer. This allowed us to quantitate tracer uptake (SUV) in the primary tumor over a standard time period (45–60 min) after injection to control for the time-dependence of the SUV. For each of 33 patients, three blood samples were collected at 55 min after FDG injection to measure plasma glucose and the glucose values averaged. The initial blood glucose determination was used in the remaining six patients. Plasma glucose levels were used to correct the FDG uptake values provided by the General Electric Advance scanner. The other thoracic field-of-view as well as the abdomen were also imaged with 10-min-long emission scans. Five-min-long emission scans were performed over the neck and pelvis. This was followed by 15-min-long transmission studies over the three fields-of-view encompassing the chest and abdomen, performed after all of the emission studies had been completed.

All of the studies were collected in two-dimensional imaging mode with scatter septae in place. Real-time randoms correction using counts obtained with a delayed coincidence window and deconvolution-based scatter corrections supplied by the manufacturer were applied. The raw PET data were reconstructed using the standard filtered back-projection available on the General Electric Advance PET system. The following reconstruction parameters were used: 12 mm Hanning filter, 55 cm image diameter, and 128 × 128 array size.

Sphere Diam. (cm)	Maximum Pixel RC
3.3	1.01
2.8	1.01
2.2	0.88
1.6	0.57
1.2	0.38
1.0	0.26
0.8	0.16
0.6	0.08
0.4	0.01

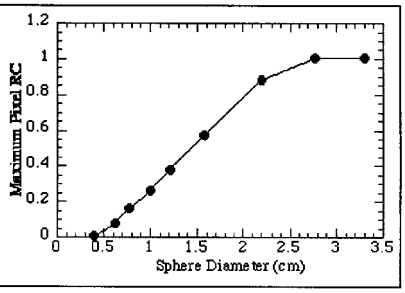

Fig. 1 Maximal pixel RCs calculated for spheres of known size and activity placed in a cold background. These spheres were imaged in the General Electric Advance PET scanner, and the images were reconstructed using the following parameters: 12 mm Hanning filter, 55 cm image diameter, and 128 × 128 array size. The maximal pixel RC is equal to the measured maximal pixel activity (provided by the PET image) divided by the known activity present in the sphere.

Quantitative Imaging Analysis. The SUV was used to quantitate tumor FDG uptake. The SUV is defined as the time-averaged tissue activity [C (μCi/ml)], from 45 to 60 min after injection, divided by the injected dose [ID (mCi)], per kg of patient body weight:

$$\mathrm{SUV}=\frac{\mathrm{C}\ (\mu\mathrm{Ci/ml})}{\dfrac{ID\ (\mathrm{mCi})}{\mathrm{weight}\ (\mathrm{kg})}} \qquad \text{(A)}$$

C is the activity at a pixel within a tissue defined by a ROI. A tumor ROI encompassing the entire lesion was placed on all of the planes in which the lesion is visualized. This was performed on the summed 45- to 60-min images. The maxSUV within the selected ROIs was used.

All of the SUV data were corrected for partial volume effects, based on the average diameter of the tumor (RCs). RCs have been estimated based on lesion diameter from phantom measurements performed in the General Electric Advance tomograph (40). These RCs have been calculated for the image reconstruction parameters and filter used in imaging of NSCLC patients (Fig. 1). These RCs (RC) were applied to the difference between lesion and background activity as defined by Eq. B. The maxSUV, instead of an average SUV over a ROI, was used because it is less sensitive to partial volume effects.

FDG uptake in normal lung background exhibits regional variations as reported by Miyauchi and Wahl (41). Normal lung FDG uptake varies from anterior to posterior lung and from apex to base but not significantly from right to left lung. Therefore, the relevant background for a NSCLC lesion was evaluated with a 6 × 6-pixel ROI adjacent to the tumor. This ROI was placed either medial or lateral to the tumor to minimize anteroposterior background variations, and away from chest wall and mediastinum. For a large tumor, the ROI was placed in the

opposite lung at a position mirroring the tumor location. This avoided placing the background ROI too close to the tumor. The average SUV over this ROI was used as the background SUV. For lesions of diameter <2.8 cm, background FDG uptake contributes to the measured tumor uptake (Eq. B) because the RC is less than 1 (Fig. 1).

$$\text{PV corrected maxSUV} = \text{background SUV} + \frac{\text{measured maxSUV} - \text{background SUV}}{\text{RC}} \quad \text{(B)}$$

Because the plasma glucose level affects the FDG SUV value, we also evaluated the PV corr maxSUV scaled as:

$$\text{gluc-PV corr maxSUV} = \text{PV corr maxSUV} \times \frac{\text{Plasma glucose level}}{100} \quad \text{(C)}$$

with blood glucose expressed in mg/dl.

The BSA implementation of the SUV was also investigated for each tumor ($n = 39$). The gluc-PV corr maxSUV was scaled to the BSA as defined in Eq. D:

$$\text{gluc-PV corr maxSUV-BSA} = \text{gluc-PV corr maxSUV} \times \frac{\text{BSA (cm}^2\text{)}}{\text{Weight (kg)}} \quad \text{(D)}$$

The BSA was calculated from height and weight according to the formula from DuBois and DuBois (42):

$$\text{BSA (cm}^2\text{)} = 71.84 \times \text{weight (kg)}^{0.425} \times \text{height (cm)}^{0.725} \quad \text{(E)}$$

These implementations of the SUV were evaluated for correlations with the Ki-67 scores and lesion size.

Surgical Staging

Thirty-seven of the 39 patients underwent complete surgical staging after FDG PET imaging. Surgical staging consisted of bronchoscopy, mediastinoscopy with or without a Chamberlain procedure or thoracoscopy. Thirty-five of these 37 patients underwent resection of their primary tumor with harvesting of accessible lymph nodes. Two surgically staged patients were unresectable (one stage IIIB, one stage IV) and had a surgical biopsy of their tumors.

The two patients that were not surgically staged consisted of: (*a*) a patient who was found to be stage IV by FDG PET imaging, with further confirmation of the metastases by magnetic resonance imaging examination. This patient underwent bronchoscopic biopsy of the primary tumor; and (*b*) a patient who underwent a percutaneous biopsy but who was not a candidate for resection because of poor medical condition (clinical stage IIIA by PET). The distribution of patients among surgical stages is reported in Table 1.

Pathology

Thirty-nine NSCLC specimens were available for pathological evaluation. Thirty-five specimens were obtained by tumor resection. Four specimens were obtained by biopsy (1 percutaneous and 3 surgical biopsies). All of the pathology material (tumor specimen and sampled lymph nodes) for each of the 39 patients was reviewed by two pathologists to assess tumor type, differentiation (poor, moderate, or well differentiated), and surgicopathological stage. A representative formalin-fixed, paraffin-embedded section from each tumor was labeled using monoclonal antibody MIB-1 (Immunotech, Westbrook, ME; 1:100) after microwave antigen retrieval in citrate buffer. Antibody binding was detected using the Vectra Elite kit with FeCl3 intensification and hematoxylin counterstain. MIB-1 recognizes the Ki-67 antigen, a 345 and 395 kDa nuclear protein common to proliferating human cells (43). The fraction of labeled tumor cells (Ki-67 score) was visually assessed over a ×4 microscopic field (3-mm diameter) in the field that contained the highest average fraction of labeled cells. The pathologists were blinded to the FDG PET results.

Statistical Analysis

Because the Ki-67 scores are numbers ranging between 0 and 100%, and not normally distributed, the nonparametric Spearman rank test was used to evaluate their correlation with tumor uptake (maxSUV). The association between tumor FDG uptake and tumor differentiation was evaluated by the Kruskal-Wallis test, a nonparametric version of one-way ANOVA.

RESULTS

For the 39 patients evaluated in this study, the following parameters were measured and are summarized in Table 1: histological subtype and tumor differentiation, surgical stage, tumor diameter, Ki-67 score, maxSUV, PV corr maxSUV, and gluc-PV corr maxSUV. For clarity, the values for the BSA definition of the SUV are not included.

The distribution of patients among surgical stages is: stage IA, 11; stage IB, 15; stage IIA, 0; stage IIB, 4; stage IIIA, 3; stage IIIB, 3; stage IV, 3 (Table 1).

For each tumor, the average lesion diameter was determined from CT scans, and the corresponding RC was applied to the lesion maxSUV while accounting for normal lung uptake (Eq. B). The correlation (Rho, 0.56; $P = 0.0006$) between uncorrected maxSUV and lesion size disappears (Rho, −0.035; $P = 0.83$) when applying the RCs. The relationship between PV corr maxSUV values and lesion diameter is shown in Fig. 2. There is also no correlation between maxSUV corrected for both partial volume and glucose (gluc-PV corr maxSUV) and lesion size: Rho, −0.047; $P = 0.77$.

Ki-67 scores, the percentage of cells positive for the MIB-1 antibody, were measured for all of the 39 NSCLC specimens. A strong correlation is found between the PV corr maxSUV and Ki-67 score of tumors: Rho, 0.73; $P < 0.0001$ (Fig. 3). Further correction for plasma glucose level (gluc-PV corr maxSUV) yielded a correlation with Ki-67 scores of: Rho, 0.67; $P < 0.0001$. The body surface area implementation of the SUV yielded the following correlation with Ki-67 scores for gluc-PV corr maxSUV-BSA: Rho, 0.645; $P < 0.0001$.

A stronger correlation between PV corr maxSUV and Ki-67 score is found for the 26 stage I lesions (11 stage IA and 15 stage IB): Rho, 0.79; $P < 0.0001$.

The other implementations of SUV have the following correlations with Ki-67 for these stage I tumors: gluc-PV corr

Table 1 Patient histology, surgical stage, tumor uptake, and Ki-67 scores

This Table summarizes the following parameters measured for the 39 patients evaluated in this study: histological subtype and tumor differentiation, surgical stage, tumor diameter, Ki-67 score, uncorrected tumor maxSUV, PV corr maxSUV, and gluc-PV corr maxSUV. For clarity, the values for the BSA definition of the SUV are not included.

Patient no.	Histology	Stage	CT diam.[a] (cm)	Ki-67	maxSUV	PV corr maxSUV	gluc-PV corr maxSUV
1	pd adenoca	IIIA	4.00	20	13.81	13.81	12.29
2	md adenoca	IB	1.10	40	2.82	7.67	7.59
3	md SCCa	IB	2.33	70	22.26	24.45	17.28
4	wd BAC	IA	1.00	5	2.92	9.19	8.85
5	md adenoca	IIB	3.20	20	7.86	7.86	7.94
6	pd SCCa	IIB	4.03	60	15.05	15.05	14.95
7	pd adenoca[b]	IB	5.33	30	11.18	11.18	12.33
8	pd SCCa	IB	2.50	30	6.42	6.78	4.54
9	pd adenoca	IA	1.03	30	7.00	24.01	22.25
10	pd large cell	IA	1.77	90	10.88	15.95	11.01
11	wd BAC	IA	1.13	5	3.21	7.27	7.27
12	pd carcinosarc	IB	4.33	50	14.56	14.56	11.36
13	pd SCCa	IA	1.20	90	7.77	19.99	18.12
14	pd large cell	IIIB	3.67	50	14.87	14.87	14.28
15	md adenoca	IA	0.70	70	2.67	17.14	16.37
16	md adenoca	IB	1.00	30	2.39	7.79	6.05
17	md adenoca	IA	2.00	80	10.03	12.67	9.80
18	wd BAC	IB	5.00	2.5	3.44	3.44	2.61
19	md adenoca	IA	1.73	40	3.85	5.68	5.68
20	md adenoca	IIB	3.40	30	7.70	7.70	6.80
21	wd BAC	IB	2.50	2.5	4.01	4.22	4.79
22	pd adenoca	IIB	1.50	50	19.92	37.24	33.39
23	md adenoca	cIIIA	5.00	70	12.64	12.64	9.23
24	pd adenoca	IV	4.83	40	9.17	9.17	8.19
25	pd large cell	IV	4.33	90	11.28	11.28	10.56
26	md SCCa	IB	3.83	20	9.27	9.27	9.02
27	wd adenoca	IB	2.73	5	3.51	3.54	3.22
28	md adenoca	IIIA	2.60	30	8.09	8.39	6.99
29	wd BAC	IB	3.70	2.5	0.55	0.55	0.59
30	pd large cell	IV	4.83	60	15.03	15.03	12.37
31	md SCCa	IIIB	3.10	50	10.68	10.68	13.03
32	pd large cell	IA	1.30	70	7.51	16.69	14.69
33	pd SCCa	IB	4.27	60	12.47	12.47	9.81
34	pd adenoca	IB	4.77	60	9.92	9.92	9.09
35	pd adenosquam	IA	1.17	70	4.60	11.80	12.74
36	md SCCa	IB	3.33	80	9.71	9.71	8.44
37	md adenoca	IA	2.17	10	4.94	5.60	4.53
38	pd large cell	IIIB	6.10	90	15.86	15.86	13.16
39	wd BAC	IB	1.80	10	1.30	1.76	1.04

[a] diam., diameter; wd, well-differentiated; md, moderately differentiated; pd, poorly differentiated; cIIIA, clinical stage IIIA (patient was not surgically staged after PET imaging); adenoca, adenocarcinoma; BAC, bronchoalveolar cell carcinoma (a subtype of adenoca); SCCa, squamous cell carcinoma; large cell, large cell carcinoma; carcinosarc, carcinosarcoma (a large cell carcinoma subtype).

[b] Clara cell type adenocarcinoma.

maxSUV: Rho, 0.715; $P = 0.0003$; and gluc-PV corr maxSUV-BSA: Rho, 0.74; $P = 0.0002$.

The best correlation between PV corr maxSUV and Ki-67 score was found for the 15 patients with surgical stage IB ($T_2N_0M_0$: Rho, 0.83; $P = 0.0019$; Fig. 4). The other implementations of SUV have the following correlations with Ki-67 for these stage IB tumors: gluc-PV corr maxSUV: Rho, 0.76; $P = 0.0047$; and gluc-PV corr maxSUV-BSA: Rho, 0.71; $P = 0.0079$. Within the cluster of the five lesions with both very low FDG SUVs and low Ki-67 scores, four are bronchoalveolar carcinomas (Fig. 4). This histological subtype of adenocarcinoma is known to have a better prognosis than other NSCLCs.

No statistically significant correlation was found between tumor size and Ki-67 score of the tumor: Rho, 0.068; $P = 0.67$ ($n = 39$ patients; Fig. 5).

A significant association was found between tumor cellular differentiation and PV corr maxSUV value ($P < 0.0001$, Kruskal-Wallis test; Fig. 6).

DISCUSSION

FDG uptake has been shown to correlate with tumor proliferative rates in lymphomas and head and neck cancers (22–26). However, such a relationship has not been definitely established in NSCLC. Our results indicate that FDG uptake in NSCLCs (quantitated as maxSUVs) correlates with cellular proliferation assessed by Ki-67 immunohistochemistry.

Both static and dynamic imaging measures of tumor FDG uptake exist: SUV *versus* FDGMR. These methods vary greatly in their level of experimental complexity. We have elected to

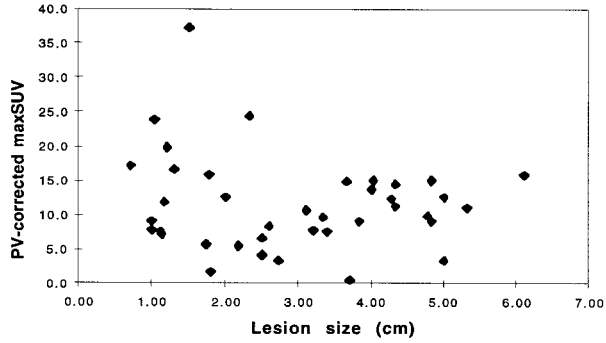

Fig. 2 Relationship between PV corr maxSUV and lesion size for the 39 NSCLCs evaluated in this study. No correlation was found between the two parameters: Rho, −0.035; $P = 0.83$.

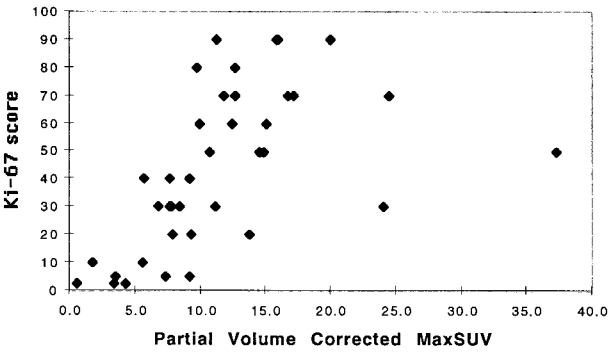

Fig. 3 A strong correlation was found between PV corr maxSUV and Ki-67 score for the 39 NSCLCs studied: Rho, 0.73; $P < 0.0001$.

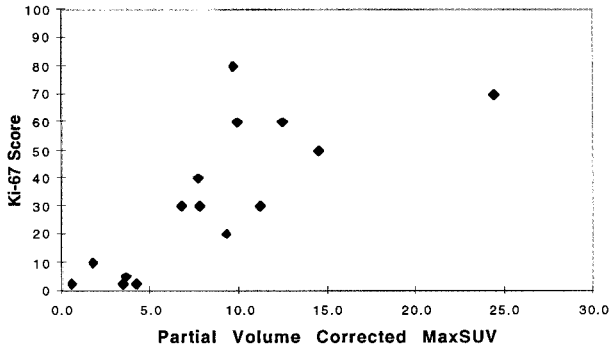

Fig. 4 The strongest correlation between PV corr maxSUV and Ki-67 score was found for the 15 stage-IB lesions: Rho, 0.83; $P = 0.0019$. Within the cluster of the five lesions with both very low FDG SUVs and low Ki-67 scores, four are bronchoalveolar carcinomas. This histological subtype of adenocarcinoma is known to have a better prognosis than other NSCLCs.

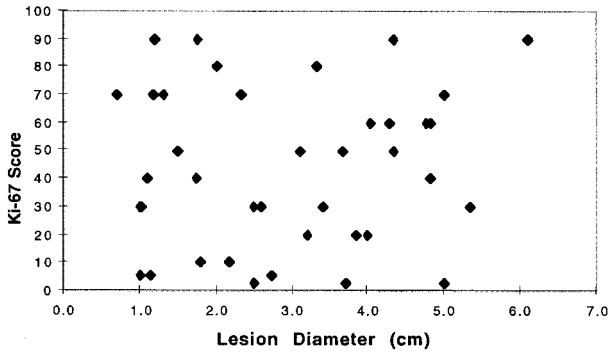

Fig. 5 Ki-67 scores plotted with respect to lesion sizes for all of the 39 lesions. No correlation is found between these two parameters: Rho, 0.068; $P = 0.67$.

quantitate FDG uptake from static imaging data and with the SUV for the following reasons: (*a*) in order for FDG uptake quantitation to have widespread application as a means of grading tumors, it needs to be simple to measure without resorting to dynamic imaging, which would limit its clinical application; and (*b*) with both tumor uptake and whole-body staging information desired for NSCLC patients, the exclusion of dynamic imaging allows for shorter imaging protocols. This helps maximize patient enrollment and compliance with the imaging protocol.

The literature evidence and our experience indicate the SUV is an adequate and simple substitute for the experimentally complex FDGMR. The experience of our PET group in FDG imaging of sarcomas has shown a high degree of correlation between the FDGMR quantitated using dynamic imaging and Patlak analysis (44) and the maximum FDG SUV of those tumors over a very wide range of metabolic rates (45). The correlation between FDGMR and FDG-SUV was better for tumors with high FDGMR values (greater than the mean of 11.7 μmol/min/100 g; *r*, 0.89) than for those with low FDGMR (*r*, 0.62). In addition, a strong correlation between SUV-lean and FDGMR (determined by dynamic imaging and graphical Patlak analysis) was found in 20 FDG PET studies performed on 10 patients with primary lung cancer (46). Similar results were also reported in head and neck cancers and lymphomas (47), and in breast cancer (48). Nonetheless, we realize that the SUV may provide less information than the FDGMR and that the SUV also increases with time after tracer injection (49, 50). For this reason, every effort was made to standardize this measurement in time with each primary lung tumor being imaged for 15 min starting at 45 min after tracer injection.

Experience with lymphomas showed that high FDG uptake, measured as a high SUV, correlates with a high S-phase fraction (26). Similarly, FDG SUV was found to correlate with the proliferative index measured by flow cytometry in head and neck tumors (23). Recently, preliminary evidence from a series of 23 patients, presented at the 1998 Society of Nuclear Medicine meeting, points to a similar correlation of FDG SUV and proliferation (measured by PCNA) in NSCLC (51). However, this study was limited mostly to lung adenocarcinomas (20 of 23 lesions), a subset of NSCLCs. This evidence suggests that the SUV represents an appropriate measure of tumor metabolism for correlation with specimen-derived markers of proliferation in NSCLC.

Tumor proliferative rates may be estimated in human tumor samples by mitotic figure counting, immunohistochemical detection of cell cycle-specific proteins (Ki-67 and PCNA), and

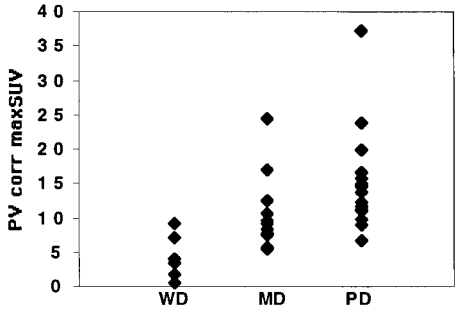

Fig. 6 Tumor PV corr maxSUVs plotted with respect to tumor differentiation at pathological review. A significant association is identified between the two variables: $P < 0.0001$ ($n = 39$). *WD,* well-differentiated; *MD,* moderately differentiated; *PD,* poorly differentiated.

DNA flow cytometry. Multiple studies provide evidence that these proliferation measures have prognostic significance in NSCLC.

A high mitotic index has been correlated with decreased survival in stage I NSCLC (6), in T_1N_0 adenocarcinomas (7), and in peripheral adenocarcinomas of less than 2-cm diameter (8). Several flow cytometry studies of NSCLC have concluded that a high S-phase fraction was a negative prognostic factor for survival (9–12). Immunohistochemical staining for Ki-67 has also been identified as a predictor of survival in NSCLC (13–16), with lower disease-free interval in patients with highly proliferating tumors (17). Increased PCNA expression was also found to predict poor outcome (18–20) and to be associated with the development of metastases (21).

We elected to make correlations between tumor FDG uptake, and Ki-67 scores of NSCLC specimens. The selection of the Ki-67 marker was made in consideration of the following: (*a*) using mitotic figure counting, immunohistochemical techniques, and flow cytometry yield results that correlate with the results of the other methods. However, the correlation coefficients are only moderately strong because of inherent difficulties with each method; (*b*) mitotic figure counting is affected by interobserver variability, use of mitotic indices *versus* mitoses per area, time between tumor resection and fixation, and the laborious nature of the analysis; (*c*) expression of cell cycle-specific proteins, such as PCNA and the Ki-67-related antigen, is easier to assess semiquantitatively; and (*d*) DNA flow cytometry is complicated by technical difficulties in obtaining nuclei for analysis, by multiple cell populations in the tumor sample whose cell cycle compartments may be inextricably intermixed, and by various methods for calculating S-phase fractions (SPF).

The tumor pixel with the highest SUV was selected to represent the overall tumor grade as it corresponds to the most metabolically active region of the tumor. A representative section of the tumor was selected and stained for Ki-67 scoring. However, the stained section may not have exactly corresponded to the area of maximal FDG uptake. In addition, tumors may exhibit regional heterogeneity with respect to their Ki-67 score. Hence, this methodology may contribute to a less-than-perfect correlation between maxSUV and Ki-67 scores. However, exact registration of maxSUV pixel with the corresponding region of the resected mass is too combersome to be implemented.

The Ki-67 score reflects the percentage of tumor cells that are stained; the nontumoral cells are not included in the population so that this method of counting corrects for the stromal fraction. However, the FDG PET scan does not correct for this stromal fraction. For example, if the tissue voxel contains a high proportion/fraction of noncancerous cells, it will decrease the SUV of this voxel. The tissues with the lowest tumor fraction but the highest Ki-67 scores are, therefore, expected to give rise to the worst correlation between Ki-67 score and maxSUV. In addition, heterogeneity in tumor fraction within a given mass could worsen this correlation. This further discrepancy is minimized by: (*a*) selecting a representative tumor sample with the highest possible tumor fraction for Ki-67 staining and scoring; and (*b*) selecting the pixel with maximal SUV from the tumor volume at PET. This should favor the selection of the voxel with the highest tumor fraction.

Our finding of a correlation between FDG uptake and Ki-67 scores in NSCLC is compatible with the report by Duhaylongsod *et al.* (36), in which FDG uptake in focal pulmonary abnormalities has been shown to correlate with lesion doubling time. Because the doubling time of a lesion reflects its rate of growth, the lesion proliferative rate would be expected to correlate with its FDG SUV. No statistically significant correlation was found in our series between the size and the Ki-67 score of a tumor. This should be expected because the size of a lesion is only a one-time measurement during its growth and does not reflect its growth rate as a proliferative score can.

The strong association present in our data between NSCLC FDG uptake and the degree of tumor cell differentiation (Fig. 6) is in keeping with prior reported results. Higashi *et al.* (52) reported a correlation between FDG uptake and degree of cell differentiation in a series of lung adenocarcinomas, with bronchoalveolar carcinomas having much lower uptake than non-bronchioalveolar carcinomas. In a series of 22 squamous cell carcinomas of the head and neck, Laubenbacher *et al.* (53) noted that higher FDG uptake was associated with decreasing cell differentiation.

The finding of a correlation between NSCLC proliferation rate and FDG uptake has prognostic implications. Proliferation markers have prognostic significance in resectable NSCLC. Therefore, the correlation found between Ki-67 scores and FDG SUV suggests that FDG uptake can be used as a noninvasive measure of tumor grade and patient prognosis. The advantage of such a measure is that it is preoperative and would allow physicians to identify those patients with resectable NSCLC who have a worse prognosis. These patients could then be treated more aggressively with the administration of neo-adjuvant chemotherapy prior to resection. Patients with less aggressive tumors and a good prognosis would undergo resection only and would be spared the morbidity and cost of preoperative chemotherapy.

Because cell differentiation is one of the parameters used in all of the tumor grading systems, the association we found between cell differentiation and FDG uptake further supports the concept of noninvasively grading NSCLCs with FDG PET. Within the cluster of the five stage IB lesions with both very low FDG SUVs and low Ki-67 scores, four were bronchoalveolar

carcinomas (Fig. 4). This histological subtype of adenocarcinoma is known to have a better prognosis than other NSCLCs. This finding is compatible with the known prognostic significance of cellular proliferation rates and with the hypothesis that FDG uptake has prognostic value.

The most significant evidence of a relationship between NSCLC FDG uptake and prognosis is in the study by Ahuja *et al.* (54). This retrospective study of FDG uptake in NSCLC showed that a SUV of >10 provided prognostic information independent of clinical stage and lesion size. However, in this study: (*a*) RCs were not used to correct for partial volume effects. Given the fact that corrections are necessary for lesions smaller than 2.8 cm imaged in the General Electric Advance scanner, the uptake of most T_1 lesions (<3 cm) was likely underestimated; and (*b*) the start of imaging time, at least 30 min after injection, was not controlled. This can result in variations in SUV.

FDG is transported into tumor cells via glucose transporter membrane proteins (Glut1–5; Refs. 55, 56). A recent study of 289 stage I NSCLCs demonstrated that increased expression of Glut1 and/or Glut3 is associated with poorer survival (57). Although not yet shown in NSCLC, Glut1 immunoreactivity was found to correlate with Ki-67 cellular proliferation scores in a group of human breast tumors (58). This evidence could provide a further link between the FDG uptake in stage I NSCLC and the prognosis and cellular proliferation.

Although the surgical stage is the most important prognostic factor to date, it provides an incomplete biological profile of NSCLC. The above results support a correlation between FDG uptake and proliferation, a known prognostic factor for NSCLC. FDG PET imaging can, therefore, provide preoperative prognostic information about the biological aggressiveness of these tumors. By helping to grade NSCLCs, FDG PET will contribute to the individualizing of patient therapy.

ACKNOWLEDGMENTS

We thank Drs. Janet Eary and Janet Rasey for helpful comments.

REFERENCES

1. Landis, S. H., Murray, T., Bolden, S., and Wingo, P. A. Cancer statistics, 1999. CA Cancer J. Clin., *49:* 8–31, 1999.

2. Mountain, C. F. Revisions in the international system for staging lung cancer. Chest., *111:* 1710–1717, 1997.

3. Asamura, H., Nakayama, H., Kondo, H., Tsuchiya, R., Shimasato, Y., and Naruke, T. Lymph node involvement, recurrence, and prognosis in resected small, peripheral, non-small cell lung carcinomas: are these carcinomas candidates for video-assisted lobectomy? J. Thorac. Cardiovasc. Surg., *111:* 1125–1134, 1996.

4. Feld, R., Rubinstein, L. V., and Weisenburger, T. H. Sites of recurrence in resected stage I non-small cell lung cancer. A guide for future studies. J. Clin. Oncol., *2:* 1352–1358, 1985.

5. Matthews, M. J., Kanhouwa, S., Pickren, J., and Robinette, D. Frequency of residual and metastatic tumor in patients undergoing curative surgical resection for lung cancer. Cancer Chemother. Rep., *4:* 63–67, 1973.

6. Harpole, D. H., Herndon, J. E., II, Young, W. G., Jr., Wolfe, W. G., and Sabiston, D. C., Jr. Stage I non-small cell lung cancer: a multivariate analysis of treatment methods and patterns of recurrence. Cancer (Phila.), *76:* 787–796, 1995.

7. Macchiarini, P., Fontanini, G., Hardin M. J., Chuancheieh, H., Bigini, D., Vignatis, S., Pingitore R., and Angeletti, C. A. Blood vessel invasion by tumor cells predicts recurrence in completely resected T1N0M0 non-small cell lung cancer. J. Thorac. Cardiovasc. Surg., *106:* 80–89, 1993.

8. Takise, A., Kodama, T., Shimosato, Y., Watanabe S., and Suemasuk, K. Histopathologic prognostic factors in adenocarcinomas of the peripheral lung less than 2 cm in diameter. Cancer (Phila.), *61:* 2083–2088, 1988.

9. Dazzi, H., Thatcher H, Hasleton, P. S., and Swindell, R. DNA analysis by flow cytometry in non-small cell lung cancer: relationship to epidermal growth factor, histology, tumour stage and survival. Respir. Med., *84:* 217–223, 1990.

10. Filderman, A. E., Silvestri, G. A., Gatsonis, C., Luthringer, D. J., Honig, J., and Flynn, S. D. Prognostic significance of tumor proliferative fraction and DNA content in stage I non-small cell lung cancer. Am. Rev. Respir. Dis., *146:* 707–710, 1992.

11. Ten Velde, G. P. M., Schutte, B., Vermeulen, A., Volovics, A., Reynders, M. M., and Blijham, G. H. Flow cytometric analysis of DNA ploidy level in paraffin-embedded tissue of non-small cell lung cancer. Eur. J. Cancer Clin. Oncol., *24:* 455–460, 1988.

12. Volm, M., Hahn, E. W., Mattern, J., Muller, T., Vogt-Moykopf, I., and Weber E. Five-year follow-up study of independent clinical and flow cytometric prognostic factors for the survival of patients with non-small cell lung carcinoma. Cancer Res., *48:* 2923–2928, 1988.

13. Tungekar, N. F., Gatter, K. C., Dunnill, M. S., and Mason, D. Y. Ki-67 immunostaining and survival in operable lung cancer. Histopathology, *19:* 545–550, 1991.

14. Scagliotti, G. V., Micela, M., Gubetta, L., Leonardo, E., Cappia, S., Borasiop, P., and Pozzi, E. Prognostic significance of Ki-67 labeling in resected non-small cell lung cancer. Eur. J. Cancer, *29A:* 363–365, 1993.

15. Pence, J. C., Kerns, B. M., Dodge, R. K., and Iglehart, J. D. Prognostic significance of the proliferation index in surgically-resected non-small cell lung cancer. Arch. Surg., *128:* 1382–1390, 1993.

16. Harpole, D. H., Herndon, J. E., Wolfe, W. G., Iglehart, J. D., and Marks, J. R. A prognostic model of recurrence and death in stage I non-small cell lung cancer utilizing presentation, histopathology, and oncoprotein expression. Cancer Res., *55:* 51–56, 1995.

17. Viberti, L., Papotti, M., Abbona, G. C., Celano, A., Filosso, P. L., and Bussolati, G. Value of Ki-67 immunostaining in preoperative biopsies of carcinomas of the lung. Hum. Pathol., *28:* 189–192, 1997.

18. Ishida, T., Kaneko, S., Akazawa, K., Tateishi, M., Sugio, K., and Sugimachi, K. Proliferating cell nuclear antigen expression and argyrophilic nucleolar organizer regions as factors influencing prognosis of surgically treated lung cancer patients. Cancer Res., *53:* 5000–5003, 1993.

19. Ebina, M., Steinberg, S. M., Mulshine, J. L., and Linniola, R. L. Relationship of p53 overexpression and up-regulation of proliferating cell nuclear antigen with the clinical course of non-small cell lung cancer. Cancer Res., *54:* 2496–2503, 1994.

20. Fontanini, G., Macchiarini, P., Pepe, S., Ruggiero, A., Hardin, M., Bigini, D., Vignati, S., Pingatore, R., and Angeletti, C. A. The expression of proliferating cell nuclear antigen in paraffin sections of peripheral, node-negative non-small cell lung cancer. Cancer (Phila.), *70:* 1520–1527, 1992.

21. Macchiarini, P., Fontanini, G., Hardin, M. J., Squartini, F., and Angeletti, C. A. Relation of neovascularization to metastasis of non-small cell lung cancer. Lancet, *340:* 145–146, 1992.

22. Minn, H., Joensuu, H., Ahonen, A., and Klemi, P. Fluorodeoxyglucose imaging: a method to assess the proliferative activity of human cancer *in vivo*. Comparison with DNA flow cytometry in head and neck tumors. Cancer (Phila.), *61:* 1776–1781, 1988.

23. Haberkorn, U., Strauss, L. G., Reisser, C., Haag, D., Dimitrakopoulou, A., Zigler, S., Oberdorfer, F., Rudat, V., and VanKaick, G. Glucose uptake, perfusion, and cell proliferation in head and neck tumors: relation of positron emission tomography to flow cytometry. J. Nucl. Med., *32:* 1548–1555, 1991.

24. Okada, J., Yoshikawa, K., Itami, M., Imaseki, K., Uno, K., Itanai, J., Kuyama, J., Mikata, A., and Arimizu, N. Positron emission tomog-

raphy using fluorine-18-fluorodeoxyglucose in malignant lymphoma: a comparison with proliferative activity. J. Nucl. Med., *33:* 325–329, 1992.

25. Reisser, C., Haberkorn, U., and Strauss, L. G. The relevance of positron emission tomography for the diagnosis and treatment of head and neck tumors. J. Otolaryngol., *22:* 231–238, 1993.

26. Lapela, M., Leskinen, S., Minn, H. R., Lindholm, P., Klemi, P. J., Soderstrom, K. O., Bergman, J., Haaparanta, M., Ruotsalainen, U., and Solin, O. Increased glucose metabolism in untreated non-Hodgkin's lymphoma: a study with positron emission tomography and fluorine-18-fluorodeoxyglucose. Blood, *86:* 3522–3527, 1995.

27. Patronas, N. J., Di Chiro, G., Kufta, C., Bairamian, D., Kornblith, P. L., Simon, R., and Larson, S. M. Prediction of survival in glioma patients by means of positron emission tomography. J. Neurosurg., *62:* 816–822, 1985.

28. Di Chiro, G. Positron emission tomography using [F^{18}]fluorodeoxyglucose in brain tumors. A powerful diagnostic and prognostic tool. Investig. Radiol., *22:* 360–371, 1987.

29. Alavi, JB., Alavi, A., Chawluk, J., Kushner, M., Powe, J., Hickey, W., and Reivich, M. Positron emission tomography in patients with glioma: a predictor of prognosis. Cancer (Phila.), *62:* 1074–0178, 1988.

30. Okada, J., Yoshikawa, K., Imazeki, K., Minoshima, S., Uno, K., Itami, J., Kutama, J., Maruno, H., and Arimizu, N. The use of FDG-PET in the detection and management of malignant lymphoma: correlation of uptake with prognosis. J. Nucl. Med., *32:* 686–691, 1991.

31. Okada, J., Oonishi, H., Yoshikawa, K., *et al*. FDG-PET for predicting the prognosis of malignant lymphoma. Ann. Nucl. Med., *8:* 187–191, 1994.

32. Holzer, T., Herholz, K., Jeske, J., and Heiss, W. D. FDG-PET as a prognostic indicator in radiochemotherapy of glioblastoma. J. Comput. Assisted Tomogr., *17:* 681–687, 1993.

33. Mineura, K., Sasajima, T., Kowada, M., Ogawa, T., Hatazawa, J., Shishido, F., and Uemura, K. Perfusion and metabolism in predicting the survival of patients with cerebral gliomas. Cancer (Phila.), *73:* 2386–2394, 1994.

34. Oshida, M., Uno, K., Suzuki, M., Nagashima, T., Hashimoto, H., Yagata, H., Shishikura, T., Imazeki, K., and Nakajima, N. Predicting the prognoses of breast carcinoma patients with positron emission tomography using 2-deoxy-2-fluoro[F-18]-D-glucose. Cancer (Phila.), *82:* 2227–2234, 1998.

35. Eary, J., Conrad, E., Bruckner, J., Folpe, A., Hunt, K. J., Mankoff, D. A., and Howlett, A. T. Quantitative [F-18]fluorodeoxyglucose positron emission tomography in pretreatment and grading of sarcoma. Clin. Cancer Res., *4:* 1215–1220, 1998.

36. Duhaylongsod, F. G., Lowe, V. J., Patz, E. F., Vaughn, A. L., Coleman, R. E., and Wolfe, W. G. Lung tumor growth correlates with glucose metabolism measured by fluoride-18 fluorodeoxyglucose positron emission tomography. Ann. Thorac. Surg., *60:* 1348–1352, 1995.

37. Arai, T., Kuroishi, T., Saito, Y., Kurita, Y., Naruke, T., and Kaneko, M. Tumor doubling time and prognosis in lung cancer patients: Evaluation from chest films and clinical follow-up study. Japanese Lung Cancer Screening Research Group. Jpn. J. Clin. Oncol., *24:* 199–204, 1994.

38. Usuda, K., Saito, Y., Sagawa, M., Sato, M., Kanmak, K., Takahashi, S., Endo, C., Chen, Y., Sakurda, A., and Fujimura, S. Tumor doubling time and prognostic assessment of patients with primary lung cancer. Cancer (Phila.), *74:* 2239–2244, 1994.

39. Tirindelli-Danesi, D., Teodori, L., Mauro, F. Modini, C., Botti, C., Cicconetti, F., and Stipa, S. Prognostic significance of flow cytometry in lung cancer. A 5-year study. Cancer (Phila.), *60:* 844–851, 1987.

40. Kohlmyer, S., Vesselle, H., Miyaoka R., Kaplan, M., and Lewellen, T. Comparison of recovery coefficients for PET based on maximum and average ROI pixel values. Eur. Assoc. Nucl. Med. Congress, Paris, Sept. 2–6, in press, 2000.

41. Miyauchi, T., and Wahl, R. L. Regional 2-[F-18]fluorodeoxyglucose uptake varies in normal lung. Eur. J. Nucl. Med., *23:* 517–523, 1996.

42. DuBois, D., and DuBois, E. F. A formula to estimate the approximate surface area if height and weight be known. Arch. Int. Med., *17:* 863–871, 1916.

43. Key, G., Becker, M. H., Baron, B. Duchrow, M., Schluter, C., Flad, H. D., and Gerdes, J. New Ki-67-equivalent murine monoclonal antibodies (MIB 1–3) generated against bacterially expressed parts of the Ki-67 cDNA containing three 62 base pair repetitive elements encoding for the Ki-67 epitope. Lab. Investig., *68:* 629–636, 1993.

44. Patlak, C., Blasberg, R., and Fenstermacher, J. Graphical evaluation of blood-to-brain transfer constants from multiple-time uptake data. J. Cereb. Blood Flow Metab., *3:* 1–7, 1983.

45. Eary, J. F., and Mankoff, D. A. Tumor metabolic rates in sarcoma using FDG PET. J. Nucl. Med., *39:* 250–254, 1998.

46. Minn, H., Zasadny, K. R., Quint, L. E., and Wahl, R. L. Lung cancer: reproducibility of quantitative measurements for evaluating 2-[F-18]-fluoro-2-deoxy-D-glucose uptake at PET. Radiology, *196:* 167–173, 1995.

47. Minn, H., Leskinen-Kallio, S., Lindholm, P., Bergman, J., Ruotsalainen, U., Teras, M., and Haaparanta, M. [F-18]Fluorodeoxyglucose uptake in tumors: kinetic *vs.* steady-state methods with reference to plasma insulin. J. Comput. Assisted Tomogr., *17:* 115–123, 1993.

48. Wahl, R. L., Zasadny, K. R., Helvie, M., Hutchins, G. D., Weber, B., and Cody, R. Metabolic monitoring of breast cancer chemohormonotherapy using positron emission tomography: initial evaluation. J. Clin. Oncol., *11:* 2101–2111, 1993.

49. Hamberg, L. M., Hunter, G. J., Alpert, N. M., Choi, N. C., Babich, J. W., and Fischman, A. J. The dose uptake ratio as an index of glucose metabolism: useful parameter or oversimplification? J. Nucl. Med., *35:* 1308–1312, 1994.

50. Keyes, J. W. SUV: standard uptake or silly useless value? J. Nucl. Med., *36:* 1836–1839, 1995.

51. Higashi, K., Seki, H., Ueda, Y., Ayabe, K., Motomura, Y., Wan, G., Taniguchi, M., Oguchi, M., Okimura, T., and Yamamoto, I. FDG uptake of non-small cell lung cancer: correlation with cell proliferation and cellular density. J. Nucl. Med., *39:* 247, 1998.

52. Higashi, K., Ueda, Y., Seki, H., Yuasa, K., Oguchi, M., Noguchi, T., Taniguchi, M., Tonami, H., Okimura, T., and Yamamoto, I. Fluorine-18-FDG imaging is negative in bronchioloalveolar lung carcinoma. J. Nucl. Med., *39:* 1016–1020, 1998.

53. Laubenbacher, C., Saumweber, D., Wagner-Manslau, C., Kau, R. J., Herz, M., Avril, N., Ziegler, S., Kruschke, C., Arnold, W., and Schwaiger, M. Comparison of fluorine-18-fluorodeoxyglucose PET, MRI and endoscopy for staging head and neck squamous-cell carcinoma. J. Nucl. Med., *36:* 1747–1757, 1995.

54. Ahuja, V., Coleman, R. E., Herndon, J., and Patz, E. F., Jr. The prognostic significance of fluorodeoxyglucose positron emission tomography imaging for patients with non-small cell lung carcinoma. Cancer (Phila.), *83:* 918–924, 1998.

55. Mueckler, M. Facilitative glucose transporters. Eur. J. Biochem., *219:* 713–725, 1994.

56. Smith, T. A. D. FDG uptake, tumor characteristics and response to therapy: a review. Nucl. Med. Commun., *19:* 97–105, 1998.

57. Younes, M., Brown, R. W., Stephenson, M., Gondo, M., and Cagle, P. T. Overexpression of Glut1 and Glut3 in stage I non-small cell lung carcinoma is associated with poor survival. Cancer (Phila.), *80:* 1046–1051, 1997.

58. Younes, M., Brown, R. W., Mody, D. R., Fernandez, L., and Laucirica, R. Glut1 expression in human breast carcinoma: correlation with known prognostic markers. Anticancer Res., *15:* 2895–2898, 1995.